1 Supplementary Information

1.1 SAXS

The 2D pattern in Figure 3 of the paper can be interpreted as follows. In the columnar phase the x-ray beam is directed parallel to the columnar director and the hexatic pattern of the inter-columnar packing can be displayed. In the solid state all the small angle reflexions are located exclusively on the vertical axis indicating that the two dimensional columnar lattice is still present. During the columnar-solid phase transition the columnar orientation is turned by 90°. Now the X-ray beam is oriented perpendicular to the director which reduces the scattering pattern of the inter-columnar structure from two to one single dimension. In the herringbone like structure the columnar stacking is kept but the cores of the disc like molecules are tilted with respect to the columnar axis. Since the X-ray is no longer parallel to the columns the intra-columnar tilt of the cores can be seen in the wide angle region. The splitting of core and chain reflexes indicates a distinct intra-columnar packing in the solid state. The different position of the reflexes could be realized by a zickzack conformation of the molecules in the columns. The tilt angle of the cores is about 30° in all cases which is also a typical value for a herringbone structure.
Figure 1 and Figure 2 show the SAXS patterns of disordered samples of the different crown ethers **1**,**4** and **2**, **3**, **5** respectively. The columnar (Δ) and solid state (○ and ☆) can be seen in each diagram.

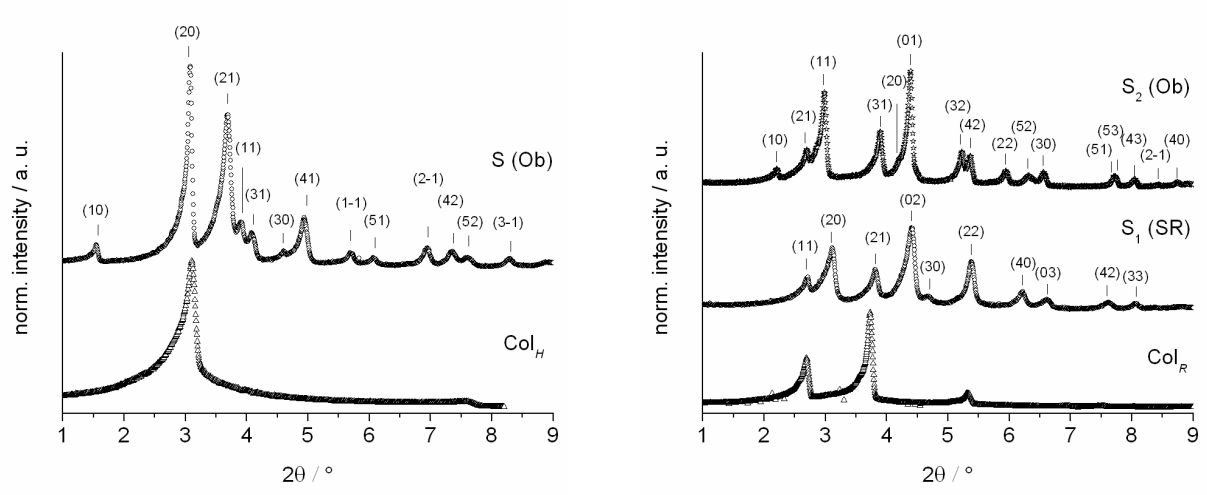

Figure 1: SAXS pattern of disordered samples of symmetric **1** and **4** in the columnar states (Δ) bottom curve and solid states S, S_1 (○) and S_2 (☆) top curve are shown.

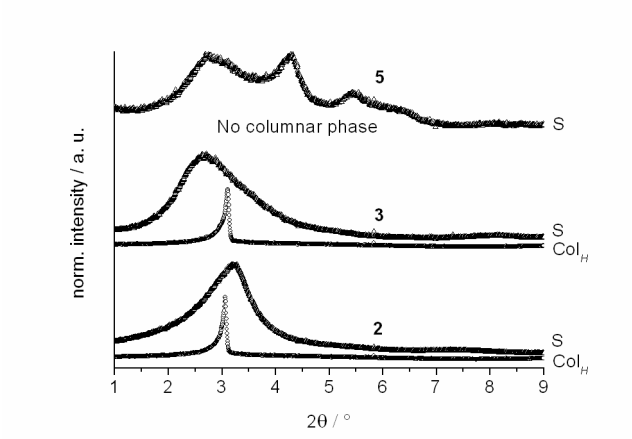

Figure 2: SAXS pattern of disordered samples of non-linear **2, 3** and **5** in the columnar states (Δ) bottom curve and solid states S (○) top curve are shown.

Non-bent **1** and **4** show sharp distict bragg reflexions in the crystalline solid state while bent shaped **2**, **3** and **5** show broad diffuse scattering peaks indicating a disordered structure.

1.2 WAXS

Figure 3 shows the WAXS pattern of disordered samples of the different crown ethers **4**, **3**, **2** and **1** (top to bottom) in the columnar liquid crystal state (left) and of **5**, **4**, **3**, **2** and **1** (top to bottom) in the solid state (right).

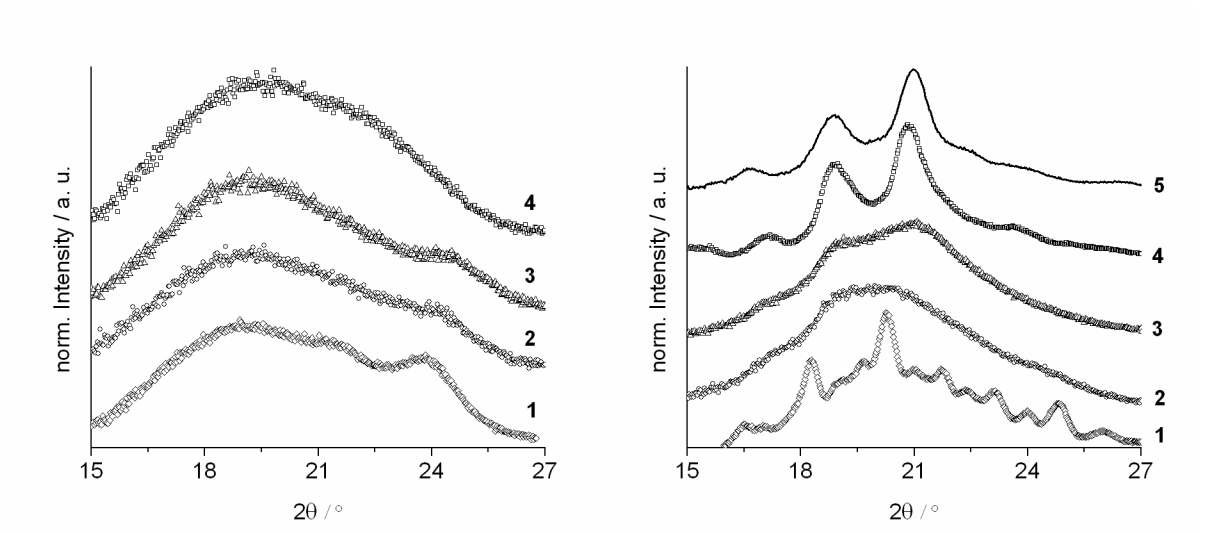

Figure 3: Wide angle diffraction of the liquid crystal phase of **4**, **3**, **2** and **1** (top to bottom) in the left plot and the solid phase of **5, 4**, **3**, **2** and **1** (top to bottom) in the right plot. In the columnar phase all compounds show a broad halo plus a shoulder in the right flank. In the solid phase symmetric **1** and **4** plus non liquid crystalline **5** show sharp reflexes while bent compounds exhibit broad diffuse reflexes.

1.3 UV-Vis

Only minor changes could be observed comparing the absorbance spectra of solid **4** and in solution (CH_2Cl_2). The absorbance bands are slightly blue shifted in solution (Figure 4).

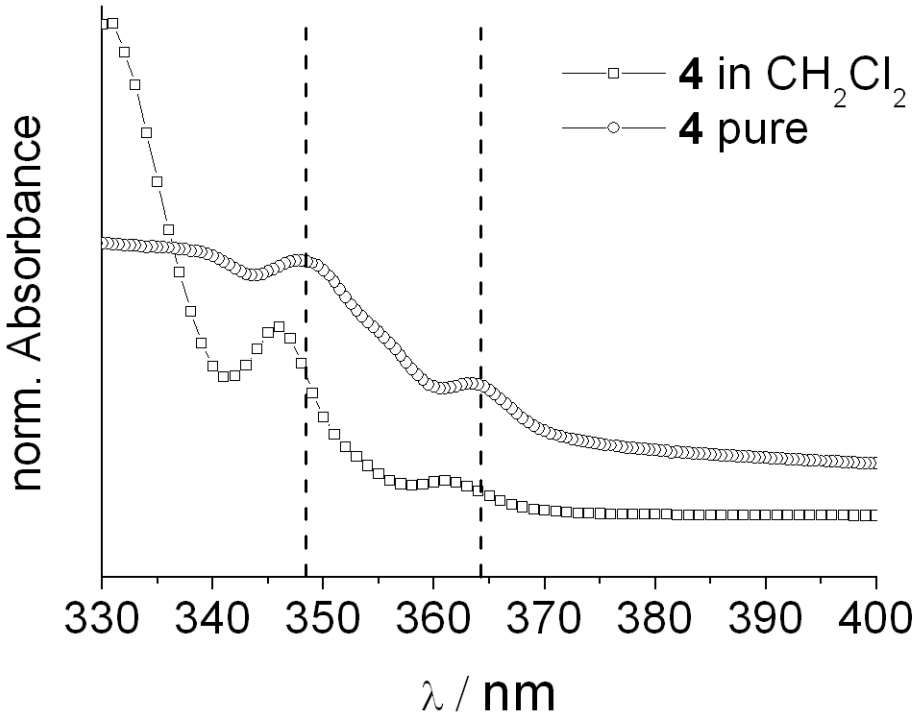

Figure 4: Absorbance spectra of solid 4 and in solution (CH2Cl2). The bands are slightly blue shifted in solution.

1.4 Isotropic State

Non-linear **2** and **3** exhibit an elevated photoconductivity in the isotropic phase compared to the insulating solid state (figure 12 paper). To investigate this strange behaviour further WAXS experiments in the isotropic phase have been carried out. It can be shown that the chain-chain correlation length according to *Scherrer* [1] stays nearly constant at the isotropic-columnar phase transition and over a wide temperature range in the columnar phase (Figure 5).

[1] H. P. Klug, (Hrsg.), *X-ray diffraction procedures*, John Wiley and sons, 1974.

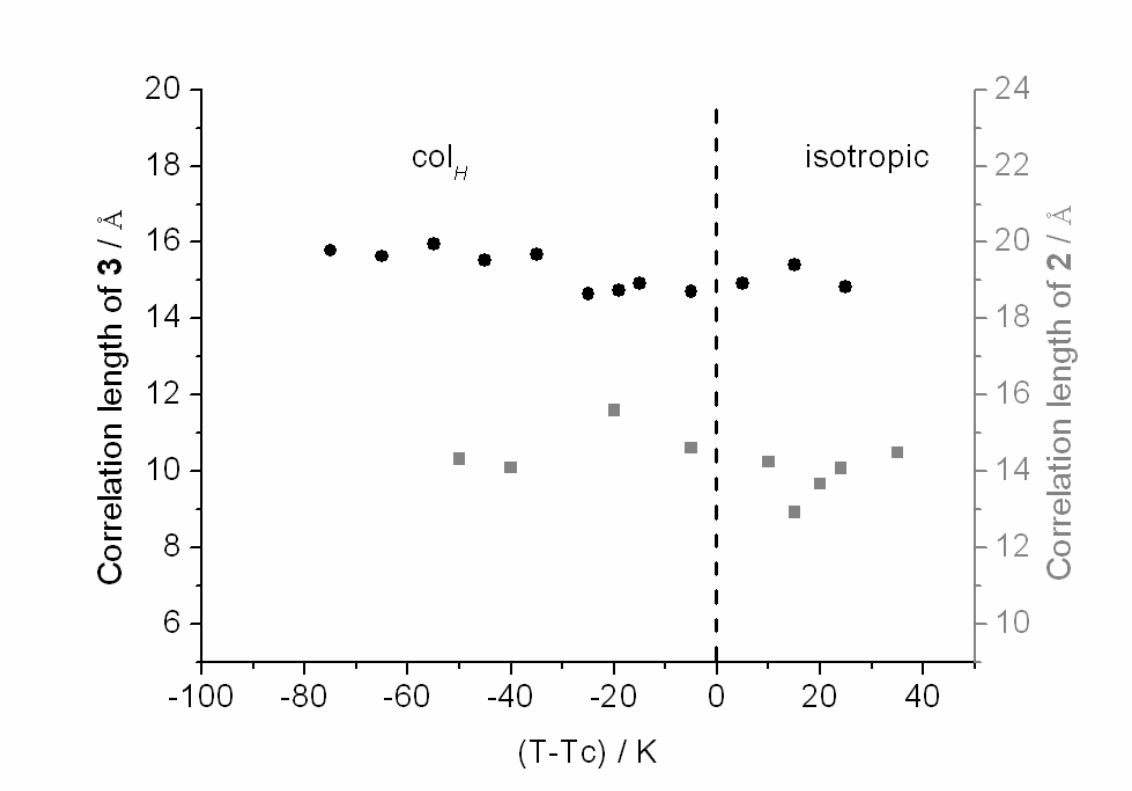

Figure 5: Temperature dependence of the correlation length of the stacks **2** (●) and **3** (■). No significant changes can be observed at the isotropic columnar phase transition.

Further cooling of the sample in the columnar phase leads to less movement of the discs in the stacks and the core-core distance appears in the flank of the halo. The inter-columnar structure is lost completely at the clearing point while the chain-chain correlation length stays close to constant. These results imply that the columns are not totally destroyed. Thus charge carriers are still able to travel short distances along the stacks and the conductivity is not cancelled completely.

1.5 OFET

Characteristic output curves are observed for all the compounds. Figure 6 shows an exemplary I_{drain} (V_{SD})-plot for crystalline **1** at 80°C. The typical linear and saturated regime depending on the gate voltage can be seen clearly.

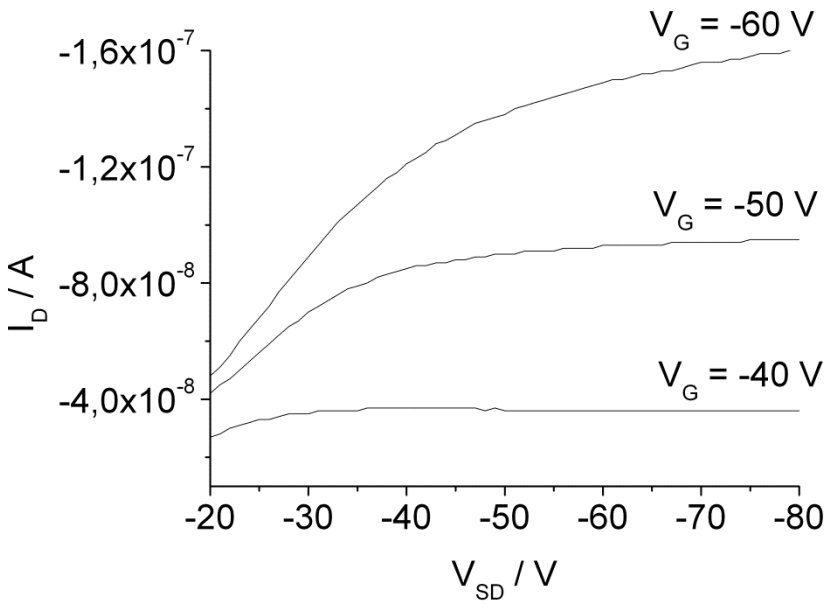

Figure 6: Characteristic output curve of crystalline **1** at 80°C. The typical linear and saturated regime can be seen, depending on the gate voltage.

To switch off the influence of different channel length or dynamic effects all different materials were measured again recording the characteristic *I-V* curves on substrates with a channel length of 5 μm. After aligning the film by mechanical shearing the samples were heated up to 10 K below the clearing point and cooled down slowly (5 $Kmin^{-1}$) to a maximum temperature of 30-40 K above the melting point to give the material the chance to self-heal possible defects. The source-drain (V_{SD}) voltage was set to -20 V (saturated region) while the gate voltage (V_G) was varied between 20 and -80 V. Before and after each measurement pictures were taken to check if the film is still intact. The results showed the same tendency as the maximum obtained mobilities mentioned above.